Some steady vortex flows past a circular cylinder

By ALAN ELCRAT[1], BENGT FORNBERG[2], MARK HORN[3]
AND KENNETH MILLER[1]

[1]Department of Mathematics, Wichita State University, Wichita, KS 67260, USA

[2]Department of Applied Mathematics, University of Colorado, Boulder, CO 80309, USA

[3]Intergraph, Huntsville, AL 35894, USA

Steady vortex flows past a circular cylinder are obtained numerically as solutions of the partial differential equation $\Delta\psi = f(\psi)$, $f(\psi) = \omega(1 - H(\psi - \alpha))$, where H is the Heaviside function. Only symmetric solutions are considered so the flow may be thought of as that past a semicircular bump in a half-plane. The flow is transplanted by the complex logarithm to a semi-infinite strip. This strip is truncated at a finite height, a numerical boundary condition is used on the top, and the difference equations resulting from the five-point discretization for the Laplacian on a uniform grid are solved using Fourier methods and an iteration for the nonlinear equation. If the area of the vortex region is prescribed the magnitude of the vorticity ω is adjusted in an inner iteration to satisfy this area constraint.

Three types of solutions are discussed: vortices attached to the cylinder, vortex patches standing off from the cylinder and strips of vorticity extending to infinity. Three families of each type of solution have been found. Equilibrium positions for point vortices, including the Föppl pair, are related to these families by continuation.

1. Introduction

We study here the classic problem of steady-state, two-dimensional inviscid flow past a bluff body. To fix ideas we have restricted attention to symmetric flow past a circular cylinder – all further discussion will be concerned with the equivalent flow in a half-space with a semicircular bump. We consider flows in which there is either a single region of constant vorticity or multiple regions in the case where the values of both the vorticity $(-\omega)$ and the stream function on the boundary of the vortex regions (α) are the same for all regions. There is a surprisingly rich structure for the possible solutions to this problem, and we believe that the clarity obtained justifies these restrictions.

Three types of vortex regions occur. These are 'attached' vortices in which the vortex region is connected to the boundary, 'isolated' vortices in which the vortex region stands away from the boundary, and 'strips' of vorticity extending to infinity along the streamline of symmetry. These three types of solutions will correspond to different choices of the value of the stream function on the boundary of the vortex. This parameter is prescribed in the partial differential equation satisfied by the stream function. The boundary of the vortex is found by observing where the stream function assumes this value.

In much recent literature, Newton's method has been used to numerically find steady although possibly time-unstable flow configurations. The numerical method

used here is unusual in that it can find such flows effectively through fast non-Newton-based iterations. The mathematical problem is here discretized using direct iteration along with a fast Poisson solver at each iteration step. In the basic algorithm that we use the vortex area is fixed and we use this as a continuation parameter in some of our computations. Area can be related to the physical parameters of circulation and vorticity, and these are used in an essential way in relating the three kinds of vortices and in mapping out the set of solutions.

Point vortices play an essential role in a part of our picture, in particular the solutions known as Föppl vortices and the translating vortex pair. Isolated vortices with circulation fixed and decreasing area are found to approach point vortices. We have found families of vortices connecting attached vortices and point vortices.

The solution method that we use might be viewed as 'vortex capturing' since no *a priori* assumption is made about the nature of the boundary of the vortex region. The iteration that we use allows arbitrary initial guesses for the vortex, and we have found only solutions in the families that we describe in our computations.

The problem of finding inviscid flows with regions of constant vorticity has been well studied, and we will not try to give any general set of references, referring the reader to the recent book Saffman (1992). On the other hand, we will mention several works that bear more or less directly on what is reported here. The solution method that we use is related to that used in Goldshtik (1963). A flow in which there may also be a vortex sheet was proposed by Taganoff and computed in Sadovskii (1971), Moore, Saffman & Tanveer (1988) and Chernyshenko (1993). Such flows in the full half-plane are generally referred to as Sadovskii flows. This model problem has great significance, in the case in which there is no vortex sheet, in studies of the large Reynolds number limit of the steady Navier–Stokes equations (Fornberg 1993), and has been computed in Pierrehumbert (1980), Saffman & Tanveer (1982) and Wu, Overman & Zabusky (1984). The inviscid flows in these references were computed using boundary integral methods for determining the boundary of a vortex, a method related to contour dynamics. It is inherent in these methods that some *a priori* assumption must be made about the vortex boundary. Variational methods can also be used. For theoretical results extensive work has been done by Burton, e.g. Burton (1989), using ideas proposed in Benjamin (1976). See also Elcrat & Miller (1991) and Fraenkel & Berger (1974). Computations have been done in Eydeland & Turkington (1988), Elcrat & Nicolio (1995), and Elcrat & Miller (1989). Results for vortex pairs in which point vortices are connected with vortices attached to the boundary have been studied in Norbury (1975) and Wu *et al.* (1984).

The paper is organized as follows. In §2 the equations to be solved are given and the numerical methods used are explained. In §3 the results for the three kinds of vortices are presented. In §4 a discussion of results is given.

2. Formulation of equations and numerical methods

Since the steady two-dimensional Euler equations are equivalent to a functional dependence between the scalar vorticity and a steam function for the flow (Lamb 1932), we may seek solutions by solving the partial differential equation

$$\Delta\psi = f(\psi) \tag{2.1}$$

for the stream function ψ, with ψ vanishing on the boundary of the body. The 'profile function' f in our assumed relationship $\omega = f(\psi)$ might be an arbitrary prescribed function or could be determined from a variational principle (Benjamin

1976; Burton 1989; Elcrat & Miller 1991). However, we will consider here only the special case $f = \omega F(\psi - \alpha)$, $F = 1 - H$, H the Heaviside function, where α and $\omega > 0$ are constants. This corresponds to a constant vorticity $-\omega$ in the region where $\psi < \alpha$, and irrotational flow elsewhere (this is in agreement with the Prandtl–Batchelor theorem describing possible limit flows for increasing Reynolds numbers). If the function f is monotone, iteration is a natural way to seek solutions of (2.1). An early implementation of this idea was made in Goldshtik (1963). In that work solutions were found that correspond to vortices attached to the boundary of a bounded domain. In a recent work, Elcrat & Miller (2000), two of the present authors have studied families of solutions that contain those of Goldshtik (1963) as well as isolated vortices and flows with non-zero vorticity on the inflow and outflow boundaries. An arbitrary monotone f was allowed. The solutions were found by applying successive approximations to (2.1), and an essential role was played by the initial guess. As in Goldshtik (1963), the successive iterants could be characterized in terms of their level sets, and the successive approximations formed a monotone sequence. In both Goldshtik (1963) and Elcrat & Miller (2000) the boundedness of the domain is required in order that the mathematical argument be carried out.

We have chosen to focus here on a single geometric configuration, the flow in a half-space past a semicircular bump. (The flow extends by symmetry to flow past a circular cylinder.) In choosing this flow domain we have eliminated the need to map out geometric dependences. The set of solutions found is rich enough to justify focusing on this single geometry; with more parameters to vary a clear presentation of results would be much more difficult. In addition, as will be seen below, we can make a simple coordinate transformation which avoids the need for mesh refinement or subtraction of singularities at corners in the flow domain in our numerical solution.

For this unbounded domain we know of no mathematical work guaranteeing the existence of solutions. Furthermore, implementing the monotone iterations described above proved troublesome and delicate: the iterated vortex regions either filled the computational domain or disappeared. We have instead used iterations in which ω is allowed to vary and the area of the vortex region is held fixed. More precisely, we solve

$$\Delta \psi_{n+1} = \omega_n F(\psi_n - \alpha), \tag{2.2}$$

where ω_n is chosen so that the area of the vortex,

$$A = |\{\psi_n < \alpha\}|,$$

is a fixed prescribed value. (This is accomplished in an inner iteration in which ω is raised or lowered to achieve the correct area in our numerical solution.) A similar idea was used in Chernyshenko (1993) in computing stratified Sadovskii flows in a channel. There circulation was fixed in the iterations instead of area. On the basis of our previous work (Elcrat & Miller 2000) we expect to obtain vortices attached to the boundary when $\alpha = 0$, isolated vortices when $\alpha < 0$, and strips of vorticity along the entire boundary when $\alpha > 0$.

We next describe the discretization of the problem.

First we transform the region in the upper half-z-plane exterior to a circle around the origin of radius 1, by the mapping $w = i \ln(z)$, to a semi-infinite strip. Since the Laplacian, Δ_z in the z-plane, transforms to $|dw/dz|^2 \Delta_w$, we can write the transformed differential equation for $\Psi(\xi, \eta) = \psi(x, y)$ as

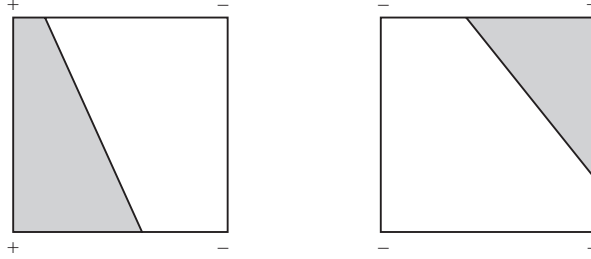$$\Delta \Psi = \omega F(\Psi - \alpha) e^{2\eta}.$$

FIGURE 1. The area of the vortex region is approximated by linear interpolation depending on the values of $\alpha - \Psi_0$ at the corners of each grid rectangle. Two of sixteen possible cases.

The boundary condition on ψ is $\psi = \psi_0$, ψ_0 the stream function for potential flow, on the boundary (where $\psi_0 = 0$) and at infinity. We can write $\psi_0 = (r - r^{-1})\sin(\theta)$ in polar coordinates in the z-plane and this transforms to $\Psi_0 = -2\sinh(\eta)\sin(\xi)$ in the w-plane, $w = \xi + i\eta$. Then $\Phi = \Psi - \Psi_0$ solves a nonlinear Poisson equation with boundary values zero on the sides and bottom of the strip $-\pi < \xi < 0$, $0 < \eta$ and at infinity.

We discretize the Laplacian with the standard five-point stencil using a uniform mesh in the w-plane. To obtain a finite problem we truncate the strip at a finite height, and apply at the top a Robin-type numerical boundary condition on the sine transform coefficients of Φ – a linear relation between $\hat{\Phi}$ and a certain discrete approximation of $\partial\hat{\Phi}/\partial\eta$ – which is exact for decaying solutions of the discrete Laplacian on the strip. The support of the vorticity in any solution obtained must be below the truncation boundary in order for this to be strictly correct. This can be checked after the fact.

The equation for Φ is solved by a form of successive approximations. This allows us to use a fast Poisson solver at each iteration step. Also we can avoid having to deal with the non-differentiability of the right-hand side, as we would have to do if a form of Newton's method were used.

A more detailed description of the algorithm will now be given. The vortex area A and α are prescribed. To start the iterative process an initial guess for Φ_0 and ω_0 is given, and the discrete version of

$$\Delta\Phi = \omega_0 \mathrm{e}^{-2\eta} F(\Phi_0 + \Psi_0 - \alpha)$$

is solved. We then calculate a discrete approximation to

$$|\{\phi < \alpha - \psi_0\}|,$$

where ϕ is the corresponding function transplanted to the physical domain. The description of the details of this are postponed for the moment. We then increase or decrease ω to get ω_1 and the corresponding $\Phi = \Phi_1$ such that

$$|\{\phi_1 < \alpha - \psi_0\}| = A \tag{2.3}$$

to within some prescribed tolerance ϵ_A. Then we begin again with Φ_1, ω_1 replacing Φ_0, ω_0. The process continues until the set of grid points where $\{\Phi_{n+1} < \alpha - \Psi_0\}$ is exactly the same as the set of grid points where $\{\Phi_n < \alpha - \Psi_0\}$. The algorithm converges approximately linearly in determining both the vortex region and the corresponding value of ω.

The calculation of areas is done by linear interpolation. On a grid rectangle there are sixteen cases corresponding to whether the grid function is greater than or less than $\alpha - \Psi_0$ at the four corners. Two typical cases are shown in figure 1. After

linear interpolation on the sides where a sign change occurs we assume that the grid function is linear in a neighbourhood of these points and calculate accordingly the appropriate area in the computational domain. The grid in the physical domain is a polar grid, so the ratio of the area of each physical domain grid 'rectangle' to the area of the corresponding computation grid rectangle can be determined exactly. We multiply by this ratio on each grid element and add over all grid elements to obtain the area $|\{\phi < \alpha - \psi_0\}|$. In our computations we have made the tolerance ϵ_A used in assessment of the required area equality (2.3) comparable to the area of one grid rectangle in the computational domain.

The numerical scheme can be summarized as follows:

(A) Specify α, the desired vortex area A, an error tolerance ϵ_A, and make an initial guess for the vortex region.

(B) Find (by bisection or the secant method) the vorticity level ω and the corresponding solution ψ_{n+1} to (2.2) so that (2.3) is satisfied with tolerance ϵ_A .

(C) If the new vortex region $\{\psi_{n+1} < \alpha\}$ differs from the previous vortex region at any grid point, return to step B.

Typically, using the secant method, item B requires about four iterations, each requiring a call to the fast Poisson solver. The number of outer iterations (returning from C to B) depends on the grid size, and is roughly proportional to the number of points along each side of the grid. For a 512 by 512 grid, 50 outer iterations are typical from a very rough initial guess. Each complete solution (with area A specified) on a 512 by 512 grid therefore typically requires around 200 calls to the fast Poisson solver. If a previously computed solution for a nearby value of A is used as an initial guess, then 10 to 15 outer iterations is more typical.

In obtaining some of the results in the next section we use a modification of this algorithm in which α instead of ω is varied. In this modification of the algorithm the Poisson equation

$$\Delta\Phi = \omega \mathrm{e}^{-2\eta} F(\Phi_n + \Psi_0 - \alpha_n)$$

is solved only once in each outer iteration. Then $\alpha = \alpha_{n+1}$ is varied so that the area equality is satisfied. The number of outer iterations for this version of the algorithm is on the same order as indicated in the previous paragraph. Since the fast Poisson solver is the most time-consuming part of the procedure, this modified algorithm is faster than the original.

The exploration of various families of solutions requires specification of other parameters, such as vorticity or circulation. The procedure above determines ω as a function of area A (for fixed α). If we wish to prescribe ω, we use a numerical equation solver to determine the corresponding A and the associated solution. Further details will be given in conjunction with the description of results.

We close this section by remarking that the basic algorithm may be thought of as formally extremizing the Dirichlet integral over functions satisfying the constraint $|\{\psi < \alpha\}| = A$. The vorticity then arises as a Lagrange multiplier for the constraint.

3. Results

We have found several families of symmetric flows past a circular cylinder by solving the equation (2.1) using the iteration and discretization described above. The general partial differential equation problem that is being solved can be expected to have many solutions, and the ones obtained depend on the set of initial guesses that we have chosen. Nevertheless, there is good reason to believe that the set of
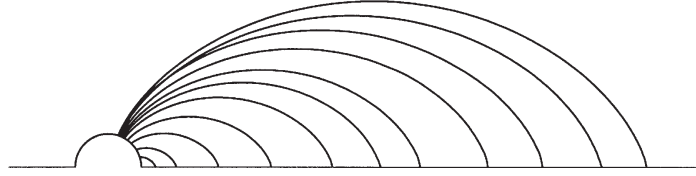
FIGURE 2. Attached ($\alpha = 0$) trailing vortices for various values of A.

all solutions possible is well represented by the set that we will give. To test this we have given initial guesses in which the vorticity is randomly distributed over the flow domain. The solutions obtained all belonged to one of the families described below.

In describing the possible solutions to equation (2.1) we note that there is a symmetry with respect to reflection across the vertical axis: if $\psi(x, y)$ solves equation (2.1), then $\psi(-x, y)$ also solves equation (2.1) for the same f. In the discussion below, for each solution in which the vortex region R is not symmetric with respect to the y-axis, there is another solution for which the vortex region is the reflection of R in the y-axis. These reflected solutions will not be explicitly mentioned below.

3.1. *Attached vortices*

For these vortices area is a convenient computational parameter. Our computations indicate the existence of vortices of arbitrarily large area behind the cylinder. Plots of the vortex boundaries for several values of A between 0.1 and 60 are given in figure 2.

We have used a computational rectangle of height π in these calculations and $h = \Delta\xi = \Delta\eta = 2^{-n}\pi$. We have tested the algorithm with n between 8 and 11 and used $n = 8$ or $n = 9$ for the graphs that appear here. The radius of the truncating boundary circle in the physical domain is then e^{π}. The boundary condition prescribed on the truncating boundary was designed so that moving the truncating boundary further out has no effect on the numerical solution, and we did experiments to verify that this is indeed the case. For a given A the computed solutions vary slightly depending on the initial guess. The deviation in the computed attachment points on the circle and on the x-axis, among the various computed solutions for a given A, was observed to be at most two grid points for $A < 15$. For $15 < A < 60$, this deviation is at most three grid points. Thus the maximum error in determining the attachment point on the circle can be estimated to be $2h$ for $A < 15$ and $3h$ for $15 < A < 60$. In determining the attachment point on the x-axis, these error estimates should be multiplied by x due to the exponential nature of the coordinate transformation in the radial direction. There is also some deviation in the computed values of ω: for $A = 20$, ω varied between 1.3358 and 1.3399 for $n = 8$, between 1.3365 and 1.3378 for $n = 9$, between 1.3368 and 1.3372 for $n = 10$, and is 1.33689 for $n = 11$.

Previous calculations of an attached vortex were made by Goldshtik (1981). He calculated the flow from a given position of the separation point on the cylinder: the point at an angle $\pi/3$ from the positive x-axis. Quantitatively our results do not agree very closely with his. Resolving the discrepancy between our results and his is difficult due to lack of information on how his results were obtained.

These attached vortex flows have a limiting nature for large A. First, the attachment point approaches the top of the circle, as suggested in figure 2. Moreover, as A increases the vortex regions appear to approach a Sadovskii vortex (without vortex sheet). The aspect ratio x_{max}/y_{max}, where x_{max} is the distance from the origin to the downstream
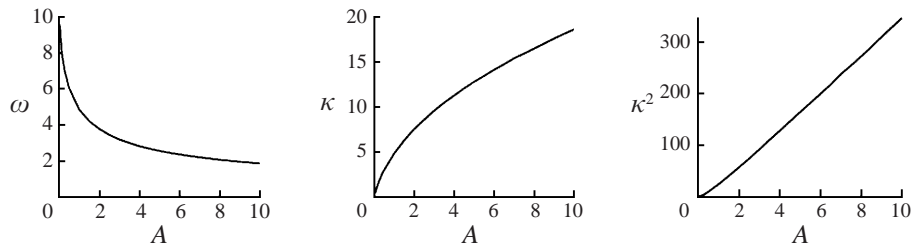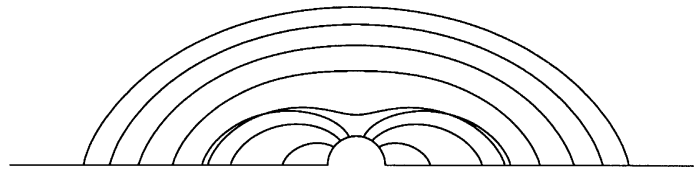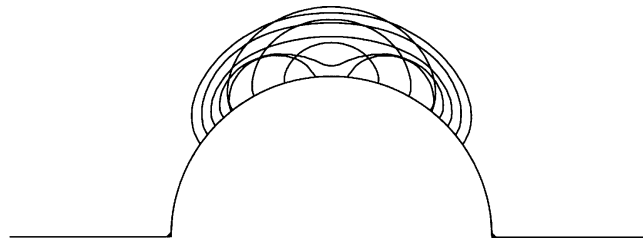
FIGURE 3. ω, κ and κ^2 as functions of A for attached trailing vortices.

FIGURE 4. Attached symmetric vortices.

FIGURE 5. Attached symmetric vortices. For each $A < 0.7$ there are two different solutions with the vortex attached to the top of the obstacle.

reattachment point, is roughly 3.3 for large areas. This compares well with the value 3.338 given in Wu *et al.* (1984), Moore *et al.* (1988) and Chernyshenko (1993) for the Sadovskii vortex.

The values of ω and the total circulation $\kappa = \omega A$ for this family are plotted as functions of area A in figure 3. The asymptotically linear relationship that appears between A and κ^2 is consistent with the fact that κ^2/A is constant for the Sadovskii vortex.

There are also two families of symmetric attached vortices. The first of these families can be parametrized by A for all positive values of A. For large A the boundary is convex and the aspect ratio asymptotically approaches the same limit as above for area tending to infinity. As A is decreased a dimple forms, and eventually (at $A \approx 15$) the vortex separates into symmetric parts as shown in figure 4. This will be discussed further below.

For small values of A there is a second family of symmetric vortices attached to the top of the circle. These are shown in figure 5. For each value of $A < 0.7$ there are two solutions in the family. At one end of the family, for $A < 0.2$ the vortex support consists of two symmetric regions. A similar looking family of vortices for non-symmetric flow past a circular cylinder with a single attached vortex (computed using boundary collocation) is given in Giannakidis (1992).

3.2. *Isolated vortices*

Before describing the isolated vortices it is helpful to note the possible stationary locations for a point vortex. The complex potential for flow past a semicircular bump of radius a in the upper half-plane with a single point vortex located at z_0 and circulation κ is given by

$$w = U\left(z + \frac{a^2}{z}\right) + \mathrm{i}\frac{\kappa}{2\pi}\log\left(\frac{z - z_0}{z - \bar{z}_0}\frac{z - a^2/z_0}{z - a^2/\bar{z}_0}\right). \qquad (3.1)$$

The condition for stationarity is

$$\frac{\mathrm{d}}{\mathrm{d}z}\left[w - \frac{\mathrm{i}\kappa}{2\pi}\log(z - z_0)\right]\bigg|_{z=z_0} = 0.$$

One set of solutions z_0, κ is given by points on $r^2 - a^2 = 2ry$ with circulation $\kappa = 4\pi Uy(1 - a^4/r^4)$. These are the well-known Föppl vortex locations shown in figure 6(*a*).

A second family of stationary point vortices can be obtained by setting $z_0 = bi$, $b > a$ in (3.1). The equation obtained reduces to

$$U\left(1 + \frac{a^2}{b^2}\right) = \frac{\kappa}{2\pi}\left(\frac{1}{2b} + \frac{2a^2 b}{b^4 - a^4}\right).$$

For any $b > a$ we can choose κ by this equation to obtain a solution. The locus is shown in figure 6(*b*). To understand the significance of this solution we can set $a = 0$, and observe that we obtain a vortex translating with speed U and circulation $4\pi bU$, another well-known set of point vortices.

In addition to these two families of single stationary point vortex locations, we note that for small κ there is a symmetric pair of stationary point vortices, each with circulation κ, with one vortex near each of the corners determined by the intersection of the circle and the x-axis (Miller 1996). The locus of such symmetric pairs can be continued to obtain the locus shown in figure 6(*c*).

For each of these stationary point vortex locations, either single vortex or symmetric pair, there is a family of isolated vortices with the same total circulation $\kappa = \omega A$ as the point vortex. To obtain each member of these families numerically we use the modification of the algorithm described near the end of §2: fix ω and let $\alpha < 0$ vary in the inner iteration in order to keep A fixed. By then increasing A incrementally with $\kappa = \omega A$ fixed, we may obtain a family of fixed-circulation vortices. Thus we have obtained three two-parameter families of isolated vortices, each parametrized by κ and α: trailing vortices desingularizing the Föppl point vortices (figure 7), connected symmetric vortices desingularizing point vortices on the y-axis (figure 8), and vortices consisting of two components which desingularize the symmetric vortex pairs (figure 9).

For A small ($-\alpha$ large) desingularizations of a point vortex have been obtained elsewhere by other numerical methods (Elcrat & Miller 1989; Eydeland & Turkington 1988). We can continue these desingularizations to maximal values of $\alpha \leqslant 0$. Our calculations indicate that for each of the Föppl point vortices the corresponding family of isolated vortices contains solutions for all values of α, $-\infty < \alpha \leqslant 0$; i.e. there is a continuous family of isolated vortices, with κ fixed, connecting the point vortex to one of the attached vortices shown in figure 2. For point vortices on the y-axis there is a κ_1 (≈ 28.5) such that for all $\kappa > \kappa_1$ the point vortex can be connected to one of the symmetric attached vortex regions shown in figure 4, and there is a
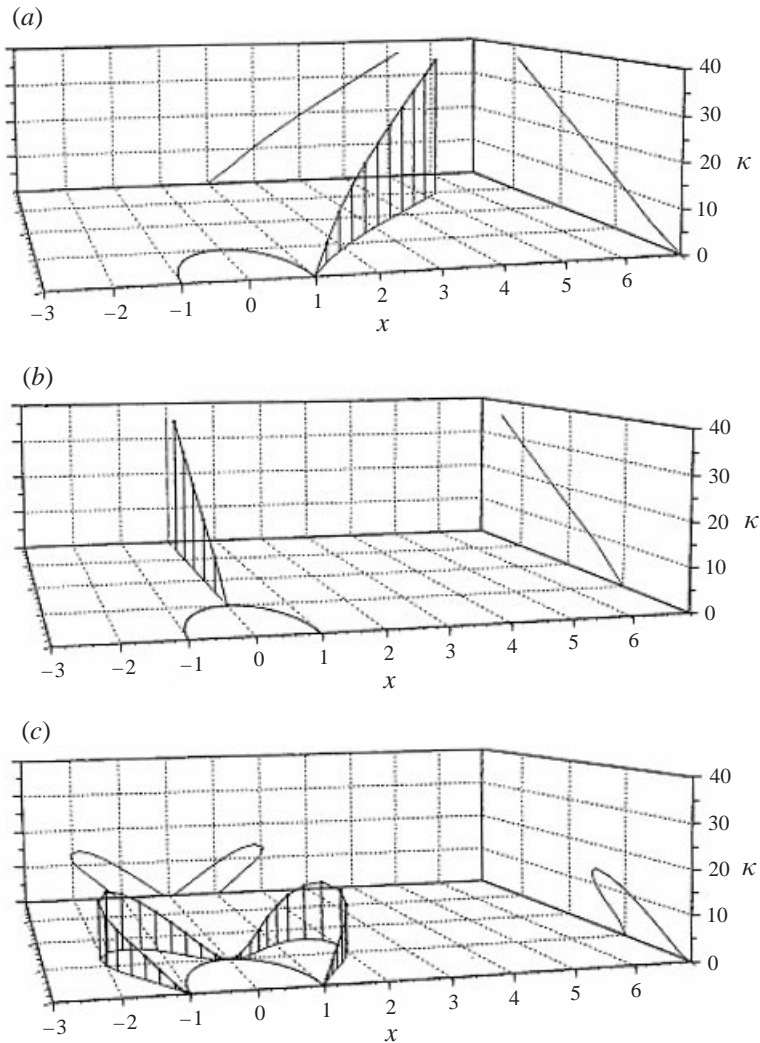
(*a*)

(*b*)

(*c*)

FIGURE 6. Point vortices. Circulation κ as a function of position for (*a*) Föppl point vortices; (*b*) point vortices on the y-axis; (*c*) symmetric point vortex pairs.
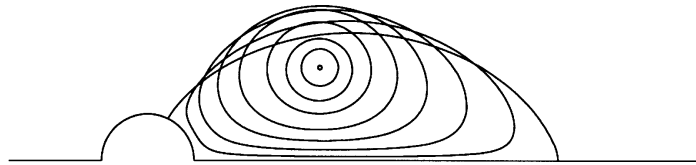

FIGURE 7. A sequence of vortex regions, with $\kappa = 25$, desingularizing a Föppl point vortex.

$\kappa_2 \, (\approx 7.8)$ such that for all $0 < \kappa < \kappa_2$ the point vortex can be connected to one of the symmetric attached vortex regions shown in figure 5, while for $\kappa_2 < \kappa < \kappa_1$ there is $\alpha_{(\kappa)} < 0$ such that the corresponding family of isolated vortices contains solutions only for $-\infty < \alpha < \alpha_{(\kappa)}$.

Symmetric point vortex pairs can likewise be joined via this continuation process to each of the disconnected symmetric attached vortices shown in figure 4. However,
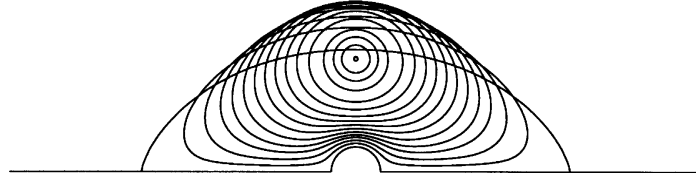
FIGURE 8. A sequence of vortex regions, with $\kappa = 50$, desingularizing
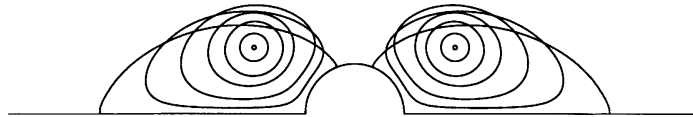a point vortex on the y-axis.

FIGURE 9. A sequence of double vortex regions, with $\kappa = 27$, desingularizing
a symmetric point vortex pair.

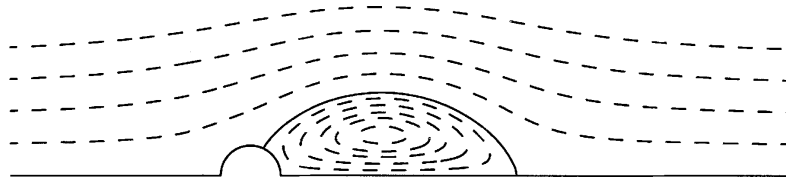

FIGURE 10. Streamline plot for the attached trailing vortex with $\kappa = 25$.

only a short range of that end of the locus of symmetric point vortices (figure 6c) which ends at the top of the circle can be desingularized all the way to an attached vortex. One such attached vortex, with two components, appears in figure 5.

Figures 10 and 11 show streamline plots for respectively the attached vortex and for a slight desingularization of the Föppl point vortex ($-\alpha$ large) with the same value of κ. In all figures the dashed lines are streamlines and the solid lines (also streamlines) represent the boundaries of the vortex regions. The wake region is definitely more elongated in attached vortex flow. Figure 12 shows streamline plots for flows near the two extremes of the family in figure 9. In this case the recirculant streamlines are not only more elongated for the attached vortex flow, but even have a different topology than in the case of the point vortex flow with the same κ.

Nearly all the isolated vortices we have found belong to one of the families just described. However it appears that not all attached vortices can be joined by a continuous constant-circulation family to a point vortex or vortex pair. The largest of the attached disconnected symmetric vortices has a circulation slightly larger than 29. For the symmetric point vortex pairs the circulation varies from 0 to about 28. For $28 < \kappa < 29$, there are isolated disconnected symmetric vortices only for $\alpha_{(\kappa)} < \alpha < 0$.

It should be pointed out that there are stationary configurations of point vortices for which we have not presented desingularizations. For example, there are unsymmetric pairs of corner vortices with $\kappa_1 \neq \kappa_2$, κ_1 and κ_2 both positive (Miller 1996). There are also configurations of three vortices, with all positive circulation, with two symmetric vortices near the corners and a third vortex on the axis. (For example, an infinitesimally weak vortex can be placed at the stagnation point above the body in figure 12(b), and its strength can then be increased.) In neither of these cases are there desingularizations which are solutions of (2.1) with $f = \omega F(\psi - \alpha)$, $F = 1 - H$ and single, global values
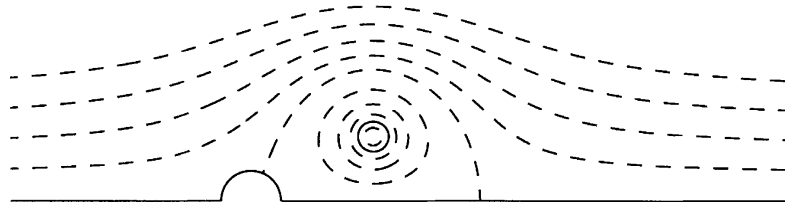
FIGURE 11. Streamline plot for trailing vortex with $\kappa = 25$ and $\alpha = -6.4$.

(*a*)

(*b*)
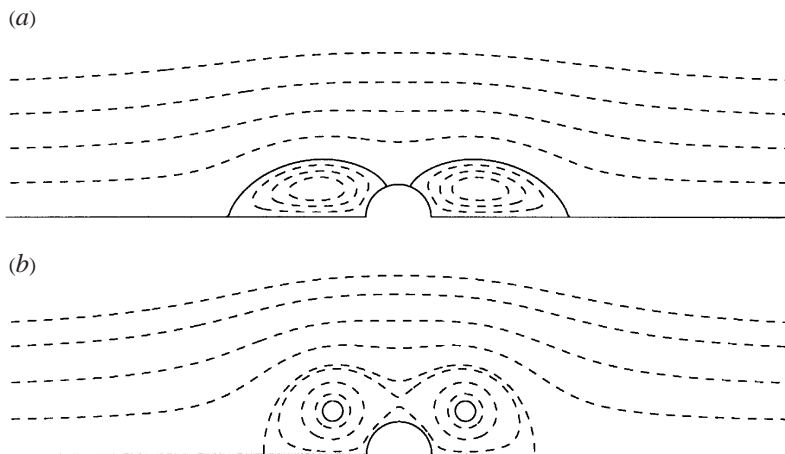
FIGURE 12. Streamline plots for two flows with the same total circulation, $\kappa = 27$.

of α and ω. In addition there are configurations of two or more point vortices with circulations of different sign (Miller 1996).

3.3. *Vortices with support extending to infinity*

These are obtained from solutions of (2.1) with $\alpha > 0$. Since the vortices are unbounded neither area nor circulation is defined. For want of a better choice, we have chosen area inside the computational domain as a computational parameter. Our basic algorithm finds ω as a function of A, but we wanted to fix the physical parameter ω. This was accomplished by making the algorithm into a Fortran function and using the equation solving routine of Brent (see Forsythe, Malcolm & Moler 1977). For some of these computations we doubled the height of the computational rectangle, which corresponds to increasing the radius of the truncating boundary circle from e^π to $e^{2\pi}$. This doubling of the computational domain resulted in no discernable change in the solution graphs in the figures that follow, but was necessary to obtain the accuracy needed in determining the relationship between α and ω in figure 14 below.

For fixed ω we have found two families of symmetric solutions for positive α. For the first of these families the limiting flow as $\alpha \to 0$ is the flow with no vortex, i.e. potential flow. This family is illustrated in figure 13(*a*).

For the second symmetric family, shown in figure 13(*b*), the $\alpha = 0$ solution is the symmetric attached vortex with the same ω. We can also find a family continued from an attached vortex behind the cylinder. This is illustrated in figure 13(*c*).

For all three families the continuation cannot be carried out past a critical value of α which depends on ω but is the same for all three families. Thus the set of all solutions appears to be connected in some sense. A graph of the maximal α as a
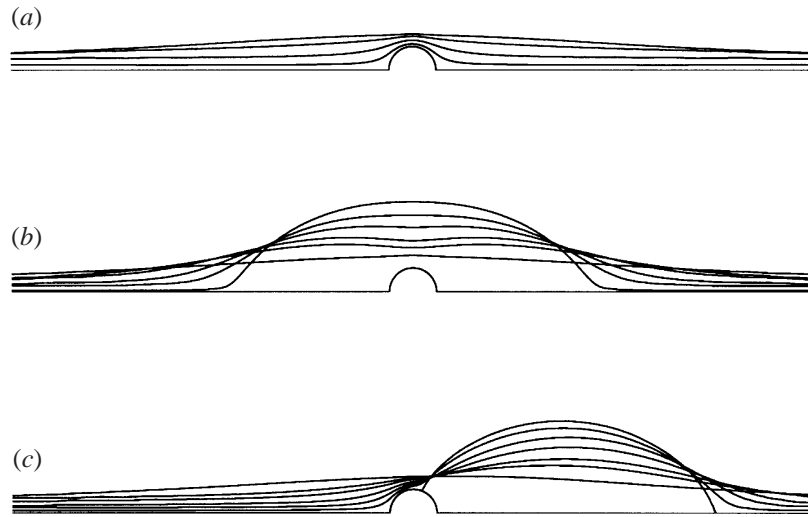
(*a*)

(*b*)

(*c*)

FIGURE 13. Three families of infinite vortices with $\omega = 1$: (*a*) perturbations of potential flow; (*b*) perturbations of a symmetric attached vortex; (*c*) perturbations of a trailing attached vortex. For all three families α varies between 0 and 0.5. The $\alpha = 0.5$ vortex region is the same for all three families.
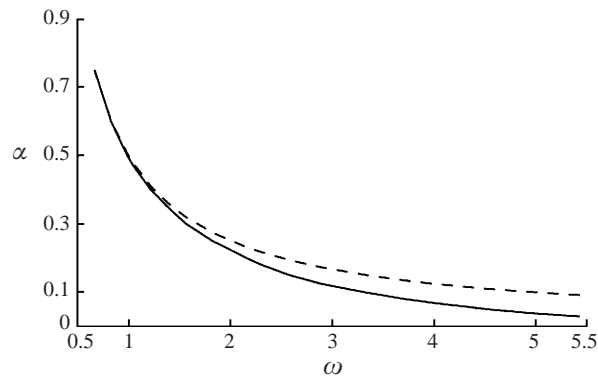
FIGURE 14. There are vortices with infinite support for parameters (ω, α) in the first quadrant below the solid curve. The dashed curve is $\alpha = 1/(2\omega)$.
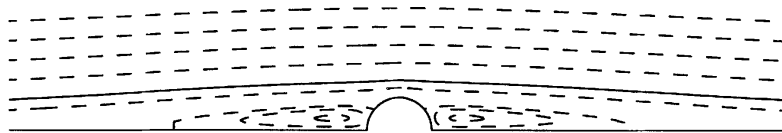
FIGURE 15. Streamline plot for the maximal α when $\omega = 1$.

function of ω is given in figure 14. Calculations indicate that each attached vortex shown in figures 2 and 4, but none of those in figure 5, can be perturbed to a flow with unbounded vortex support.

A streamline plot for the solution for the maximal value of α is given in figure 15. It appears that for all $\alpha > 0$ there is recirculation near each of the corners where the semicircle intersects the x-axis. For the first of these families these regions of
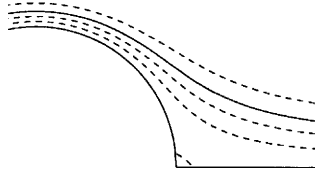
FIGURE 16. The $\alpha = 0.2$ solution from the first $\omega = 1$ family shows
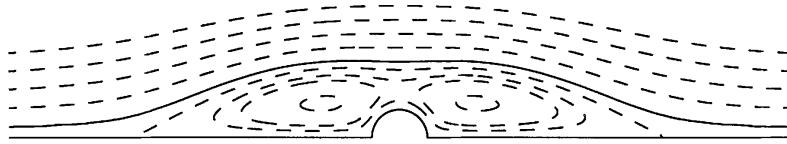a small recirculation region in the corner.

FIGURE 17. Streamline plot for the second family of infinite vortices with $\omega = 1$, $\alpha = 0.3$.
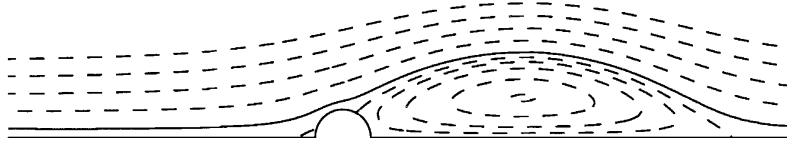

FIGURE 18. Streamline plot for the unsymmetric vortex with $\omega = 1$, $\alpha = 0.25$.

recirculation may be very small, as in figure 16. For the second family the region of recirculating flow gets smaller as α increases. Figure 17 shows a typical streamline plot. For the unsymmetric family (figures 13c and 18), as α increases the recirculation region behind the semicircle gets smaller while the recirculation region in front increases until symmetry is reached at the maximal value of α.

Analysis of the corresponding flows when there is no circle may help shed some light on our observations concerning these vortices. For the upper half-plane the stream function ψ for such flows will be given by

$$\psi = \begin{cases} u_w y + \frac{1}{2}\omega y^2, & \psi < \alpha, \\ Uy + k, & \psi > \alpha, \end{cases}$$

where the constant u_w is the velocity along the x-axis and U is the potential flow velocity. Differentiability of ψ implies that $u_w^2 = U^2 - 2\alpha\omega$. Taking $U = 1$, it follows that there are two solutions for $\alpha < 1/(2\omega)$. (Figure 14 shows that the set of (α, ω) for which there are solutions with positive α is nearly the same with or without the circular obstacle for $\omega < 1$, the presence of the obstacle restricting the range of α as ω increases.) The solutions with $u_w > 0$ and $u_w < 0$ correspond respectively to the first and second families of solutions shown in figure 13. The third family in figure 13 arises from the matching of a solution from the first family in the far-field upstream with a solution from the second family in the far-field downstream, the presence of the obstacle causing a change in the direction of the flow along the x-axis. This provides some explanation of the perhaps surprising fact that all three families (four counting the reflection of the third family) come together at the same maximal α.

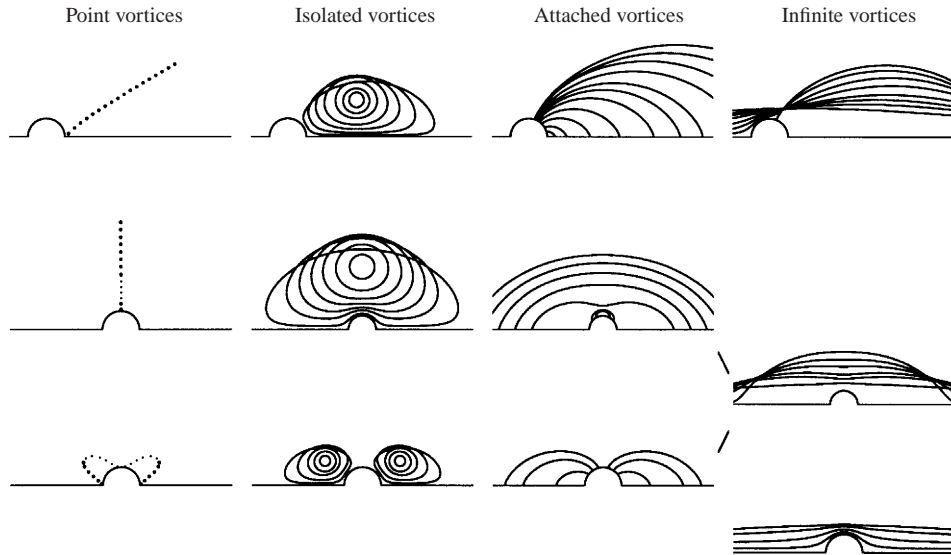Point vortices Isolated vortices Attached vortices Infinite vortices

FIGURE 19. One-parameter families of point vortices and attached vortices and related two-parameter families of isolated and infinite vortices. The third family of infinite vortices are perturbations of potential flow.

4. Discussion

An attempt has been made to give a complete catalogue of single vortex flows past a semicircular bump in a half-space. Figure 19 gives a summary of the solutions we have obtained. Each stationary single point vortex or symmetric point vortex pair can be desingularized to a family of isolated vortices ($\alpha < 0$) with the same circulation. In many cases (for those point vortices in the ranges indicated by larger dots in figure 19) the resulting family of fixed-circulation isolated vortices can be continued to an attached vortex ($\alpha = 0$). Except for the small family of vortices which are attached entirely to the semicircle (those in figure 5), each attached vortex can be perturbed to a family of unbounded vortices for a certain range of $\alpha > 0$.

The limiting flow if viscosity tends to zero for steady, viscous flow past a circular cylinder is believed to be a scaled version of Sadovskii flow with length and width proportional to the Reynolds number (Fornberg 1985; Chernyshenko 1988; Chernyshenko & Castro 1993). The possible role of the flows described here as intermediate cases in this limit or as the result of such things as blowing or suction in the viscous flow lie outside the scope of this paper.

The tools we have used can be generalized in many directions. Other shapes than a circle and finite dimensions for the flow domain can be introduced. This requires only a different conformal mapping and a careful treatment of possible singularities of the stream function at corners of the flow domain in order that numerical accuracy be retained. Asymmetry and/or multiple vortices require a more general algorithm. In particular, multiple area constraints will have to be simultaneously satisfied if several vorticities are to be obtained. We plan to return to this interesting problem.

As discussed in Elcrat & Miller (2000), the corresponding axisymmetric problem lends itself to similar methods.

REFERENCES

BENJAMIN, T. B. 1976 The alliance of practical and analytic insights into the nonlinear problems of fluid mechanics. In *Applications of Methods of Functional Analysis to Problems in Mechanics.* Lecture Notes in Mathematics, vol. 503, pp. 8–29. Springer.

BURTON, G. R. 1989 Variational problems on classes of rearrangements and multiple configurations for steady vortices. *Ann. Inst. H. Poincare Anal. Non-Lineaire* **6**, 295–319.

CHERNYSHENKO, S. I. 1988 The asymptotic form of the stationary separated circumfluence of a body at high Reynolds number. *Appl. Math. Mech.* **52**, 746. (*Transl. from Prikl. Matem. Mekh.* **52**, 958–966.)

CHERNYSHENKO, S. I. 1993 Stratified Sadovskii flow in a channel. *J. Fluid Mech.* **250**, 423–431.

CHERNYSHENKO, S. I. & CASTRO, I. P. 1993 High-Reynolds-number asymptotics of the steady flow through a row of bluff bodies. *J. Fluid Mech.* **257**, 421–449.

ELCRAT, A. R. & MILLER, K. G. 1989 Computation of vortex flows past obstacles with circulation. *Physica* D **37**, 441–452.

ELCRAT, A. R. & MILLER, K. G. 1991 Rearrangements in steady vortex flows with circulation. *Proc. Am. Math. Soc.* **111**, 1051–1055.

ELCRAT, A. R. & MILLER, K. G. 2000 A monotone iteration for concentrated vortices. *Nonlinear Analysis* (to appear).

ELCRAT, A. R. & NICOLIO, O. 1995 An iteration for steady vortices in rearrangement classes. *Nonlinear Anal., Theory Meth. Applics.* **24**, 419–432.

EYDELAND, A. & TURKINGTON, B. 1988 A computational method of solving free-boundary problems in vortex dynamics. *J. Comput. Phys.* **78**, 194–213.

FORNBERG, B. 1985 Steady viscous flow past a circular cylinder up to Reynolds number 600. *J. Comput. Phys.* **61** 297–320.

FORNBERG, B. 1993 Computing steady incompressible flows past blunt bodies – A historical overview. In *Numerical Methods for Fluid Dynamics* (ed. P. G. Baines & B. R. Morton). Oxford University Press.

FORSYTHE, G., MALCOLM, M. & MOLER, C. 1977 *Computer Methods for Mathematical Computations.* Prentice Hall.

FRAENKEL, L. E. & BERGER, M. S. 1974 A global theory of steady vortex rings in an ideal fluid. *Acta Mathematica* **132**, 13–51.

GIANNAKIDIS, G. 1992 Problems of vortex sheets and vortex patches. Dissertation, Imperial College of Science, Technology and Medicine, London.

GOLDSHTIK, M. A. 1963 A mathematical model of separated flows in an incompressible liquid. *Sov. Phys. Dok.* **7**, 1090–1093.

GOLDSHTIK, M. A. 1981 *Vortex Flows.* Nauka, Novosibirsk.

LAMB, H. 1932 *Hydrodynamics.* Cambridge University Press.

MILLER, K. G. 1996 Stationary corner vortex configurations. *Z. Angew. Math. Phys.* **47**, 39–56.

MOORE, D. W., SAFFMAN, P. G. & TANVEER, S. 1988 The calculation of some Batchelor flows: the Sadovskii vortex and rotational corner flow. *Phys. Fluids* **31**, 978–990.

NORBURY, J. 1975 Steady planar vortex pairs in an ideal fluid. *Commun. Pure Appl. Maths* **38**, 697–700.

PIERREHUMBERT, R. T. 1980 A family of steady translating vortex pairs with distributed vorticity. *J. Fluid Mech.* **99**, 129–144.

SADOVSKII, V. S. 1971 Vortex regions in a potential stream with a jump of Bernoulli's constant at the boundary. *Appl. Math. Mech.* **35**, 729 .

SAFFMAN, P. G. 1992 *Vortex Dynamics.* Cambridge University Press.

SAFFMAN, P. G. & SZETO, R. 1981 Structure of a linear array of uniform vortices. *Stud. Appl. Maths* **65**, 223–248.

SAFFMAN, P. G. & TANVEER, S. 1982 The touching pair of equal and opposite uniform vortices. *Phys. Fluids* **25**, 1929–1930.

WU, H. M., OVERMAN, E. A. & ZABUSKY, N. 1984 Steady-state solutions of the Euler equations in two dimensions: rotating and translating V-states with limiting cases. I. Numerical algorithms and results. *J. Comput. Phys.* **53**, 42–71.